Amit I, Levitin N, Gadrich M, Ben-Mayor M, Wyant T, Barak R, et al. Negative Feedback Expansion of Tregs Caused by Endogenous IL-2 Limits the Activity of IL-2-based Therapies. J Cancer Immunol. 2023;5(1):29-39.

Supplementary Materials

Supplementary Figures

A.

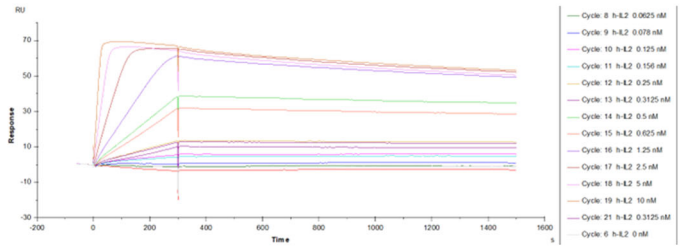

KD (M)	1.08E-11
Koff (1/s)	4.87E-04
ka (1/Ms)	4.50E+07
Chi² (RU²)	0.1

B.

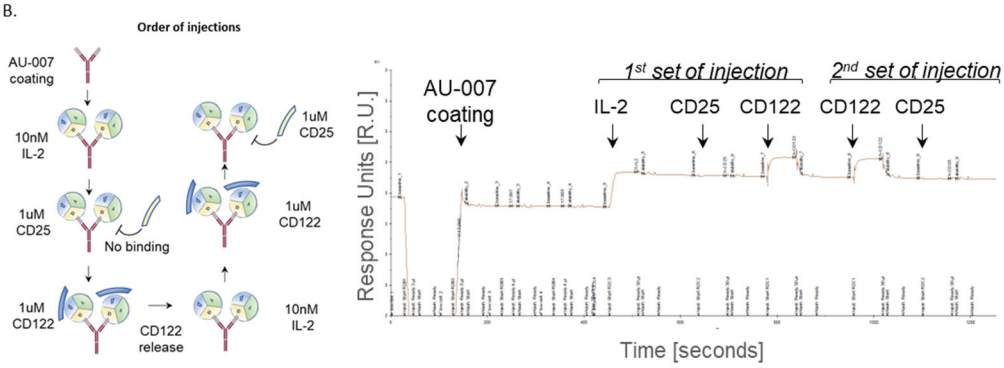

C.

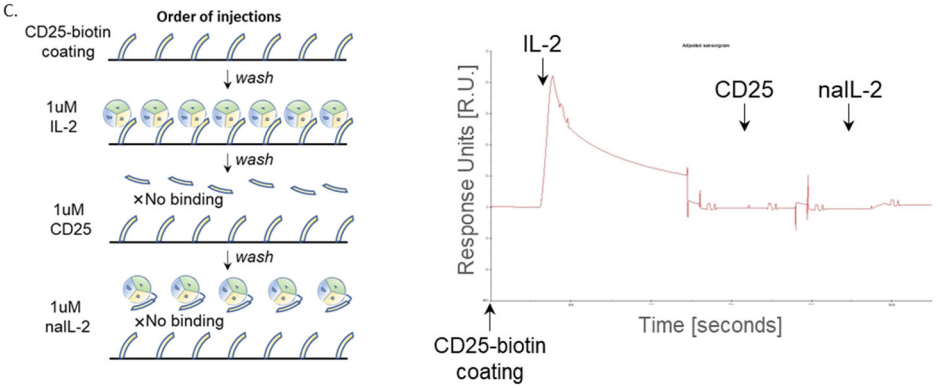

D.

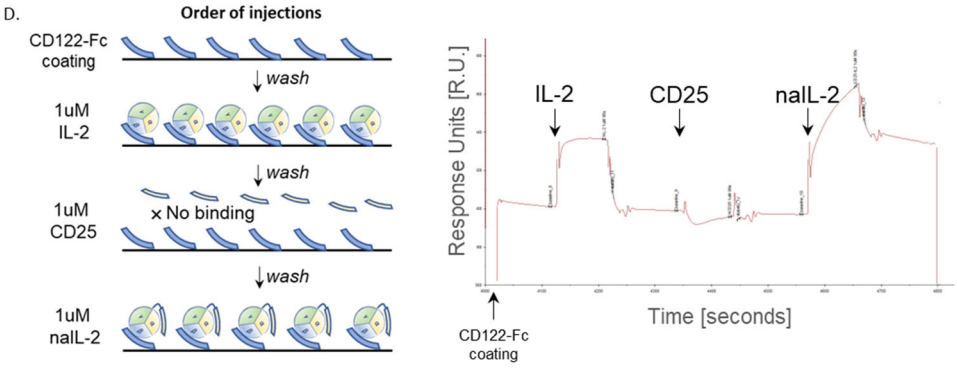

Amit I, Levitin N, Gadrich M, Ben-Mayor M, Wyant T, Barak R, et al. Negative Feedback Expansion of Tregs Caused by Endogenous IL-2 Limits the Activity of IL-2-based Therapies. J Cancer Immunol. 2023;5(1):29-39.

Figure S1. A-B: *AU-007 binds human IL-2 with high affinity and inhibits the binding to hCD25 while preserving the binding to hCD122.* Affinity and epitope binding site was assessed using Surface Plasmon Resonance (SPR). A. SPR sensorgram traces and calculated binding kinetics of a CM5 chip-bound AU-007 with hIL-2 serving as analyte. B. AU-007 Epitope binding analysis: AU-007 was captured on a CM5 chip and soluble hIL-2 was injected, forming a complex. Subsequently, soluble hCD25 was injected followed by the injection of soluble hCD122. Diagrams represent SPR sensorgram traces of complex formation of Ab/IL-2/IL-2R. Arrows indicate where hIL-2, hCD25, and hCD122 were injected. **C-D:** naIL-2 (*hIL-2/hCD25 conjugate) inhibits the binding to hCD25 while preserving the binding to hCD122.* C. Biotinylated hCD25 was captured on a CM5 chip and soluble hIL-2, soluble hCD25, and naIL-1 were injected subsequently. D. Fc tagged hCD122 was captured on a CM5 chip and soluble hIL-2, soluble hCD25, and soluble naIL-2 were injected subsequently. Diagrams represent SPR sensorgram traces of complex formation of IL-2R/Cytokine. Arrows indicate where hIL-2, hCD25, and hCD122 were injected.

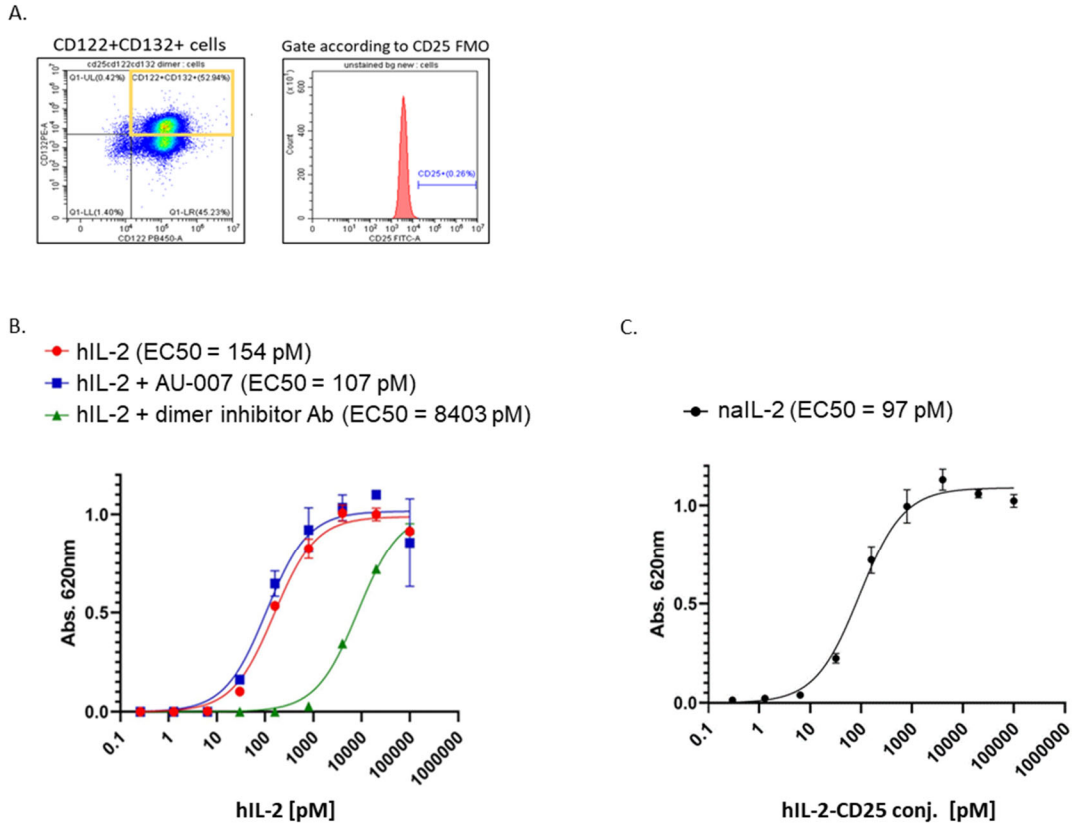

Figure S2. AU-007 and the naIL-2 do not hinder CD122/CD132-STAT5 signaling activity. A HEK239-dimer-STAT5-SEAP reporter cell line that stably expresses the human IL-2 dimer receptor (CD122/CD132) with no expression of CD25 and drives the expression of secreted embryonic alkaline phosphatase (SEAP) under a STAT5 promoter, was used to detect IL-2/IL-2-dimeric receptor signaling. A. CD25, CD122, and CD132 expression levels were detected using flow cytometry verifying the exclusive expression of the dimeric receptor. B. Dose response curves of IL-2 alone (red circles) or in the presence of 200nM AU-007 (blue squares) or of 200nM of an anti-IL-2 antibody that inhibits interactions with the dimeric receptor (green triangles). C. Dose response curve of naIL-2 (black circles). HEK239-dimmer-STAT5-SEAP reporter cells were treated with increasing concentrations of hIL-2 alone or with indicated anti-hIL-2 antibodies (B) or with increasing concentrations of naIL-2 (C), 24h post-treatment accumulated levels of SEAP were measured from cells media and functional EC-50 was calculated using GraphPad (B & C).

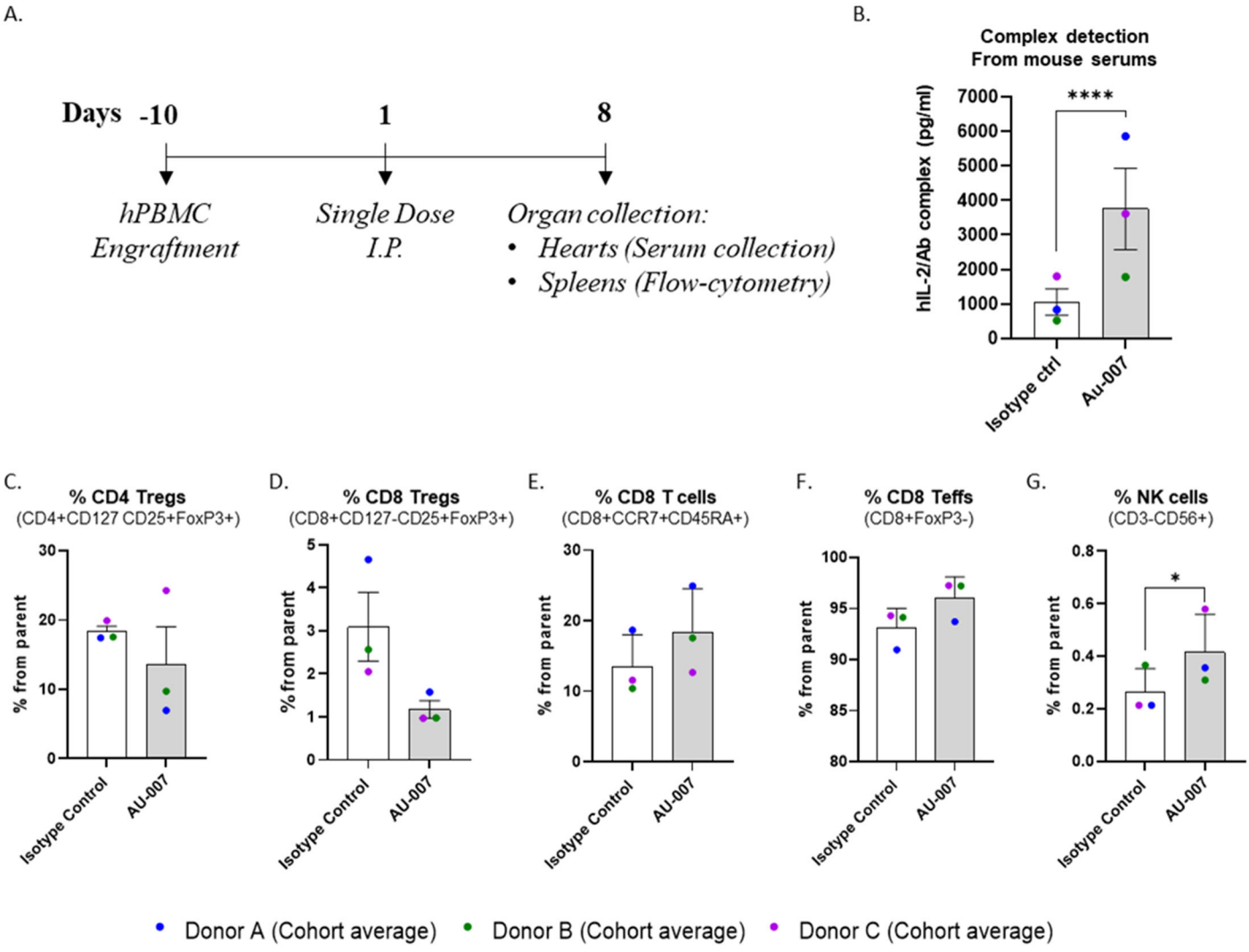

Figure S3. AU-007 captures endogenous IL-2 and demonstrates in-vivo potent immune-stimulating effects even 8 days after a single treatment. NOG-EXL mice were engrafted with hPBMCs from 3 human donors to examine donor-to-donor variability. 10 days post hPBMCs engraftment mice were randomized to the study groups (9 mice per cohort, each composed of 3 mice from each donor, colored dots represent the average of each donor for every cohort). Study groups mice were treated once with 20mg/Kg AU-007 or with 20mg/Kg of isotype control Ab (hIgG1-LALA), no exogenous IL-2 was added. A. Experiment outline. B. AU-007/hIL-2 complex detection from mouse serum using ELISA n=9±SD. C-G: Immune cell analysis of splenocytes using flow cytometry n=9±SE. Human immune cells were defined from total lymphocytes as hCD45+hCD3+, and subpopulations were defined using anti-human antibodies as indicated. Statistical analysis was done using the 2way ANOVA test, * $p < 0.05$, **** $p < 0.0001$.

Supplementary Tables

Table S1. *Antibodies used for flow cytometry in vitro experiments of cultured hPBMCs.*

Markers	Fluorochrome	Clone	Cat.	Isotypes	Vender
hCD3	PE- CF594	UCHT1	562280	Mouse IgG1, κ	BD
hCD4	FITC	RPA-T4	555346	Mouse IgG1, κ	BD
hCD8	APC-Cy7	RPA-T8	557760	Mouse IgG1, κ	BD
hCD25	BV421	BC96	302630	Mouse IgG1, κ	BioLegend
hCD127	BV711	HIL-7R-M21	563165	Mouse IgG1, κ	BD
hCD56	BV605	HCD56	318334	Mouse IgG1, κ	BioLegend
hFoxP3	PE	150D/E4	12-4774-42	Mouse IgG1, κ	eBioscience
pSTAT5	AF647	47/Stat5(pY694)	562076	Mouse IgG1, κ	BD
Viability dye	EF660	NA	65-0864-18	NA	eBioscience

Table S2. *Antibodies used for flow cytometry experiments of hPBMCs that were isolated from spleens of NOG-EXL mice engrafted with hPBMCs.*

Markers	Fluorochrome	Clone	Cat.	Isotypes	Vender
mCD45	PerCP-Cy5.5	30-F11	103132	Rat IgG2b	BioLegend
hCD45	BV785	HI30	304048	Mouse IgG1, κ	Biolegend
hCD3	BUV395	SK7	564001	Mouse BALB/c	BD
hCD4	FITC	OKT4	317408	Mouse IgG2b, κ	BioLegend
hCD25	BV711	M-A251	356138	Mouse IgG1, κ	BioLegend
hCD127	PE-Cy7	HIL-7R-M21	560822	Mouse IgG1, κ	BD
hFoxP3*	PE	259D/C7	560082	Mouse BALB/c	BD
hCD8	PE/Dazzle594	SK1	344744	Mouse IgG1, κ	BioLegend
hCD45RA	BV421	HI100	304130	Mouse IgG2b, κ	BioLegend
hCCR7	APC	G043H7	353214	Mouse IgG2a, κ	BioLegend
hCD56	BV605	HCD56	318334	Mouse IgG1, κ	BioLegend
Viability dye	eF780	NA	65-0865-18	NA	eBioscience